Conjugate Heat Transfer Analysis Model for Best Estimation of In-Vessel Retention of Multiple Layered Corium

Jae-ho Bae*, Jong-Woon Park
Dongguk univ., 707, Seokjang-Dong, Gyeong Ju, South Korea
** Corresponding author: jae2143@naver.com*

1. Introduction

In-vessel corium retention (IVR) by external reactor vessel cooling (ERVC) as shown in Fig. 1 is a favorable severe accident management and thus has been studied for decades. In order for the IVR to be successful, the heat flux at the outer surface of the vessel should be less than critical heat flux (CHF) or vessel failure can occur by focused heat load from the metal layer especially in the case of high-power reactors. Therefore, the focusing effect has been regarded as a critical issue for successful IVR.

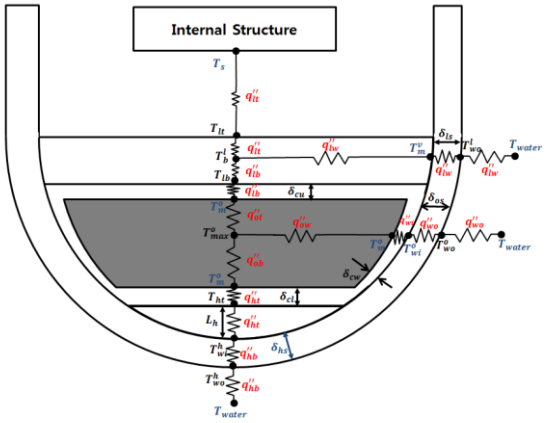

Fig. 1. Three-layered corium thermal-resistance model.

The heat transfer mechanism for the configuration shown in Fig. 1 is a coupled conjugate heat transfer problem consisting of the corium natural convection, three-dimensional (3D) conduction through the massive reactor vessel and boiling heat transfer at the external surface of the vessel. Although the heat flux from the light metal layer has been regarded as an important factor in the IVR evaluation, one more important thing to be carefully treated is the massive reactor vessel itself in that it has a strong effect of heat diffusion which alleviates focused heat load from the top metallic region to the lower temperature regions at the upper cylindrical part and lower hemispherical part. Therefore, even though the heat flux from the top metal layer to the vessel inside is larger than CHF, it might not be so at the external surface.

Heat transfer problem of the IVR with ERVC needs a set of models for the three-layered corium, the crust, the reactor vessel and the external cooling. Individual models to be found from the literature are those by Theofanous et al. [1], Esmaili and Khatib-Rahbar [2] and Zhang et al. [3]. All these models did not consider 3D conjugate heat transfer through the vessel or neglected heat transfer from the oxide pool to the lower heavy metal layer.

Present paper tries to find a solution to said light metal layer issue of the IVR by using an integrated conjugate heat transfer analysis method with fine 3D heat conduction in a reactor vessel. The present model, as shown in Fig. 1, calculates the steady-state three-dimensional (3D) temperature distribution of the vessel through coupled computations with in-vessel three-layered corium stratification and the polar-angle dependent boiling heat transfer at the outer surface of the vessel. In order to evaluate the accuracy of the present corium model, thermal load, the remaining vessel thickness and crust thickness are compared with previous calculations. The 3D vessel wall conduction analysis is validated against the FLUENT code [4].

2. Method and Analysis

2.1 In-Vessel corium Three-Layered Model

The melt configuration assumes a stratified molten pool consisting of a heavy metallic bottom layer, an oxide pool in the middle and a light metal layer on the top. The model assumes a fully molten ceramic material in the oxide pool and no existence of uranium metal in the light metal layer. As shown in Fig. 1, the present three-layered corium model uses a lumped-parameter thermal-resistance circuit heat transfer analysis method.

Heat balance equations of each layer area are as follows:

- Light metallic layer

$$Q_l'''V_l + q_{l,b}''A_{l,b} = q_{l,t}''A_{l,t} + q_{l,w}''A_{l,w} \quad (1)$$

- Middle Oxide Pool

$$Q_o'''V_o = q_{o,t}''A_{o,t} + q_{o,w}''A_{o,w} + q_{o,b}''A_{o,b} \quad (2)$$

- Bottom heavy metal layer

$$q_{h,t}''A_{h,t} + Q_h'''V_h = q_{h,b}''A_{h,b} \quad (3)$$

For the light metal layer and the oxide pools, the convective heat flux to each directions are as follows:

$$q_l'' = h_J(T_K - T_L) \quad (4)$$

Nomenclature

A	Area, m^2
$c_{p,l}$	Water specific heat at constant pressure, W/kg
g	Gravitational acceleration, m/s^2
F	Multiplier to simulate boiling conditions
h	Heat transfer coefficient, W/m^2-K
h_{boil}	Nucleate boiling heat transfer coefficient, W/m^2-K
h_{trans}	Transition boiling heat transfer coefficient, W/m^2-K
h_{film}	Film boiling heat transfer coefficient, W/m^2-K
h_{fg}	Heat of vaporization for water, W/kg
k	Thermal conductivity, W/m-K
L_h	Characteristic length of heavy metal
N_r	Number of radial nodes
Nu	Nusselt number
Pr	Prandtl number
Q'''	Volumetric heat generation rate, W/m^3
q''	Average heat flux, W/m^2
R	Vessel inner radius
Ra	Rayleigh number
Ra'	Modified Rayleigh number
T	Temperature, K
T_b^l	Bulk temperature of light metal layer, K
T_m^o	Melting temperature of oxide pool, K
T_m^v	Melting temperature of vessel wall, K
T_{max}^o	Maximum temperature of oxide pool, K
ΔT_{sat}	$T_w - T_f$
V	Volume, m^3
δ	Thickness, m
ε	Emissivity
σ	Stefan–Boltzmann constant
σ_l	Liquid surface tension, N/m
θ	Polar angle along hemispherical lower head
θ_p	Maximum Polar angle

Superscripts

cyl	Cylindrical vessel part
h	Heavy metal layer
l	Light metal layer
o	Oxide pool
sph	Hemisherical vessel part

Subscripts

c	Oxide crust
cu	Upper oxide crust
cl	Lower oxide crust
cw	Sidewall oxide crust
dn	Downward
h	Heavy metal layer
hb	Bottom surface of heavy metal layer
hs	Vessel wall in heavy metal layer
ht	Top surface of heavy metal layer
I,J,K,L	Indices for corium layers and crusts
i,j	Indices of nodes of the vessel
l	Liquid
lb	Bottom surface of light metal layer
ls	Vessel wall in light metal layer
lt	Top surface of light metal layer
lw	Sidewall of light metal layer
o	Oxide pool
ob	Bottom surface of oxide pool
os	Vessel wall in oxide pool
ot	Top surface of oxide pool
ow	Sidewall of oxide pool
s	Vessel upper internal structure
v	Vapor
f	External water
w	Vessel wall
wi	Inside of vessel wall
wo	Outside of vessel wall

where h_J stands for convective heat transfer coefficients through each heat flow directions from the two pools as shown in Fig. 1. The heat transfer coefficients, h_J, that are potentially applicable to the metallic and the oxide pools, respectively, are summarized in Ref. 3.

For the heavy metal at the bottom, Esmaili and Khatib-Rahbar [2] assumed the oxide lower crust and the heavy metal layer is insulated. Therefore, the heat flux to the bottom surface of the heavy metal layer is estimated simply using only the volumetric heating inside the heavy metal with $q_{ht}'' = 0$ in Eq.(5). However, it should be noted that this assumption could be misleading since the insulation assumption has no physical basis. In the present model, the heat transfer is thus estimated by:

$$q_{hb}'' = (Q_h''' V_h + q_{ht}'' A_{ht})/A_{hb} \quad (5)$$

Also, since the heavy metal occupies little volume and the downward heat flow from the upper oxide pool is generally lower than the upward heat flow, the heavy metal is assumed to be solid (this will be confirmed after integral calculation) and thus following heat conduction may hold:

$$q_{ht}'' = \frac{k_h}{L_h}\left(T_{ht} - T_{wi}^h\right) \quad (6)$$

The radiative heat transfer from the upper surface of the light metal layer to the upper remaining structures inside the reactor vessel or to the vessel internal surface is found by:

$$q_{lt}'' = \sigma(T_{lt}^4 - T_s^4)\left[\frac{1}{\varepsilon_{lt}} + \frac{1-\varepsilon_s}{\varepsilon_s}\frac{A_{lt}}{A_s}\right]^{-1} \quad (7)$$

Assuming 1D conduction though the crust, following equation can be applied:

$$q_I'' = \frac{k_I}{\delta_I}(T_L - T_M) \quad (8)$$

The convection from the external surface of the vessel is given by following heat balances:

$$q_I'' = h_I(T_I - T_f) \quad (9)$$

In Eqs.(8) and (9), *I* stands for each location of the corium layers and *L* and *M* are inner and outer temperatures of the crust or the vessel.

2.2 Thermal Load Correlations along Polar Angle

The local downward heat flux along the side surface of the oxide pool is obtained from the heat flux distribution as a function of the angular position. For this, the Theofanous correlation for the mini-ACOPO facility [1] is used as follows:

$$\frac{q_{dn}''(\theta)}{q_{dn}''} = \frac{Nu_{dn}(\theta)}{Nu_{dn}} = 0.1 + 1.08\left(\frac{\theta}{\theta_p}\right) - 4.5\left(\frac{\theta}{\theta_p}\right)^2 + 8.6\left(\frac{\theta}{\theta_p}\right)^3, 0.1 \le \frac{\theta}{\theta_p} \le 0.6 \quad (10a)$$

$$\frac{q_{dn}''(\theta)}{q_{dn}''} = \frac{Nu_{dn}(\theta)}{Nu_{dn}} = 0.41 + 0.35\left(\frac{\theta}{\theta_p}\right) + \left(\frac{\theta}{\theta_p}\right)^2, \quad 0.6 \le \frac{\theta}{\theta_p} \le 1.0 \quad (10b)$$

2.3 External Water Boiling Model

The external reactor vessel cooling (ERVC) is the final aspect of the heat transfer from the corium through the lower head to the surroundings. For the nucleate boiling regime of the external water, the Nusselt number of the Rohsenow [5] is assumed:

$$Nu = \frac{1}{{C_{sf}}^3}\left(\frac{c_{p,l}\Delta T_{sat}}{h_{fg}Pr_l}\right)^2 \quad (11)$$

where C_{sf} is constant depending on the surface on the roughness and the wettability. The boiling heat transfer coefficient h_{boil} is thus expressed as:

$$h_{boil} = \left(\frac{g[\rho_l - \rho_v]}{\sigma_l}\right)^{1/2}\left(\frac{c_{p,l}}{h_{fg}C_{sf}Pr_l}\right)^3(\mu_l h_{fg})(\Delta T_{sat})^2 \quad (12)$$

2.4 Vessel Wall Conduction and Solution Procedure

The present solution procedure is two-step and tightly linked with the wall conduction calculations. For this, 1D and 3D conduction equations are needed for the vessel part. To solve the lumped thermal resistance equations in the previous sections, following 1D conduction equations are used:

$$q_I'' = \frac{k_I}{\delta_I}(T_I - T_M) \quad (13)$$

where *I* stands for each location of the corium layers and *L* and *M* are inner and outer temperatures of the vessel.

As a first step, coupled equations from (1) to (9), and (13) are solved by using the Newton-Raphson numerical method imbedded in MATLAB [6] to obtain lumped and interface temperatures and the thicknesses shown in Fig. 1, the polar angle dependent heat flux $q''(\theta)$ to the vessel internal surface is obtained from Eq.(9).

As a second step, this heat flux $q''(\theta)$ and local external boiling heat transfer rate obtained by using Eq.(12) is imposed as inner and outer conjugate boundary conditions to the 3D conduction equations: they are r-φ-θ steady-state heat conduction equation for the hemispherical lower head and r-φ-z equation for the upper cylindrical part. The central finite-difference method is applied to each analytic equation and obtained from general discretized equations of Ref. 7.

The conjugate boundary conditions at the vessel inner and outer surfaces are imposed as follows:

$$q_j'' = k_w\frac{T_{1,j,k}^{sph} - T_{2,j,k}^{sph}}{\Delta r} \quad (14a)$$

$$k_w\frac{T_{N_r-1,j,k}^{sph} - T_{N_r,j,k}^{sph}}{\Delta r} = \left(\frac{g[\rho_l - \rho_v]}{\sigma_l}\right)^{\frac{1}{2}}\left(\frac{c_{p,l}}{h_{fg}C_{sf}Pr_l}\right)^3 \times (\mu_l h_{fg})\left(T_{N_r,j,k}^{sph} - T_f\right)^2 \quad (14b)$$

In Eq.(14b), $T_{N_r,j,k}^{sph}$ appears at the left and right hand sides and they are nonlinear so iteratively solved. Throughout the iterations, it is assumed that the reactor vessel is solid state even though temperature is partially increased beyond its melting temperature. This assumption is unphysical but would give sufficient insight on the 3D heat diffusion effect of the vessel.

Numbers of nodes used are 40 in the radial direction, 960 in the polar angle direction of the hemispherical part and 613 in the axial direction of the cylindrical part.

2.5 Critical Heat flux correlation

The lower bound critical heat flux correlation obtained by Theofanous et al. for the Configuration III test facility [1] is as follows:

$$q_{cr}'' = A_{CHF} + B_{CHF}\theta + C_{CHF}\theta^2 + D_{CHF}\theta^3 + E_{CHF}\theta^4 \quad (15)$$

where the coefficients can be found from Theofanous et al. [1].

3. Results and discussion

3.1 Accuracy of the Separate Models

Three-layer corium model

In order to verify the present corium model, separate analyses are conducted for the AP1000 reactor condition presented in Table 1 previously used by Esmaili and Khatib-Rahbar [2]. Two combinations of light and heavy metals are considered as shown in Table 1.

Table 1: Input data for the AP1000 reactor

Parameter	Value
Reactor vessel inner radius (m)	2.0
Reactor pressure vessel thickness (m)	0.15
Oxide pool mass (ton)	88.5
Light metal layer mass (ton)	30/26
Heavy metal mass (ton)	0.03/4.0
Oxide pool decay power (MW)	14.3
Oxide crust decay power (MW)	0
Heavy metal layer decay power (MW)	0

Firstly, discussion for a case with light metal mass of 30 tons and a very small amount of heavy metal (0.03 ton) will be made to compare with the results of Esmaili and Khatib-Rahbar [2]. The present calculation results of heat flux from each layer, vessel remaining thickness and crust thickness profiles are compared with the three calculations by Esmaili and Khatib-Rahbar [2] and they are shown in Figs. 2 to 4. In these figures, the abbreviations T and B3D stand for Theofanous [1] and BALI-3D [8] Nusselt number correlation for oxide pool, respectively. Also, Tm and G stand for Theofanous [1] and Globe-Dropkin [9] correlation, respectively. For the sideward heat transfer from the light metal, Churchill-Chu [10] correlation is used.

The present calculation is performed by trial and error to find best agreement to the previous calculations of the Esmaili and Khatib-Rahbar [2] and the best agreement is obtained with the Nusselt correlations of B3D-G combination.

The heat flux profiles in Fig. 2 show that all the calculations are close to each other between polar angle from 40 to 76 degrees. The slight difference out of this region comes from the basic difference of the present formulations from Esmaili and Khatib-Rahbar [2]. The best-fit correlations in the present model are different from T-Tm combinations used by Esmaili and Khatib-Rahbar [2].

Figure 3 shows the vessel remaining thickness from the present 1D and 3D predictions. The remaining thickness is obtained by eliminating the regions with temperatures higher than 1750 K. Present 1D calculation agrees well to the previous calculations below the metallic region. However, the difference is larger for the metallic regions and this is naturally due to differences of heat fluxes between those calculations in Fig. 2. However, it can be stressed from Fig. 3 that the 3D vessel conjugate heat transfer calculation provides largest vessel remaining thickness at the metallic region due to heat diffusion along the polar angle. Figure 4 shows that the present prediction of the oxide crust thickness is in good agreement with previous calculations.

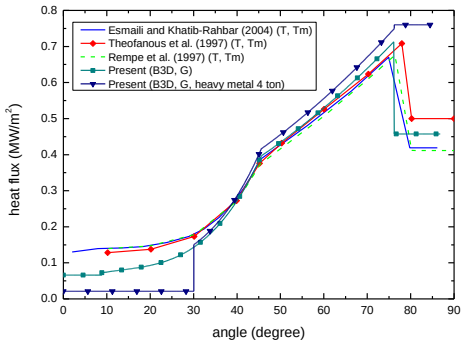

Fig. 2. Comparison of heat flux..

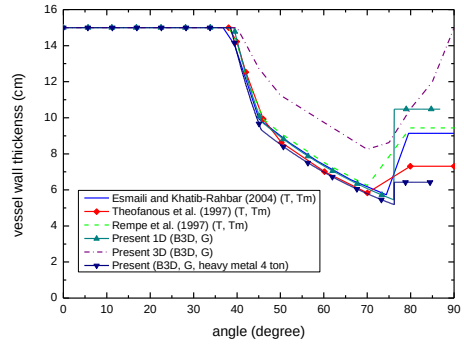

Fig. 3. Comparison of vessel wall thickness.

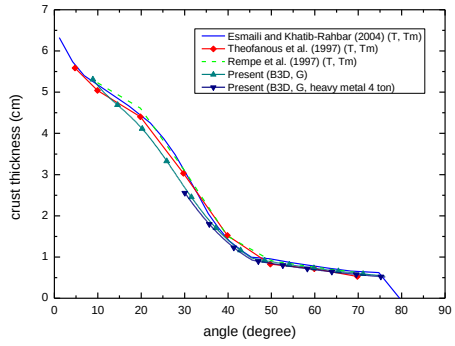

Fig. 4. Comparison of crust thickness.

Sensitivity calculation for 4.0 tons of heavy metal mass and light metal mass of 26 tons shows that the polar angle of the oxide pool bottom increases to 30 degrees due to increased mass of the heavy metal (see Fig. 2). The heat flux from the light metal layer greatly increases from 0.46 to 0.76 MW/m^2 due to

reduction of the light metal mass. With respect to the heat flux from the heavy metal layer, the heat flux is discontinuous from the upper oxide region heat flux in the same way as between the oxide pool and the light metal layer. This is because the present lumped corium model provides only single values of the heat fluxes from the heavy and light metal layers whereas the heat flux correlation of Eq.(10) for the oxide pool gives polar angle dependent heat flux.

Due to increased heat flux from the light metal layer, the vessel remaining thickness decreases from 10.3 cm to 6.3 cm as shown in Fig. 3. On the other hand, the variation of oxide crust thickness is negligible as shown in Fig. 4 since the heat flow from the upper oxide region to the heavy metal layer is independent of the heavy metal mass.

Reactor Vessel 3D Conduction for Constant Outer Wall Temperature

In order to find the validity of the present 3D vessel heat conduction analysis, temperature contour obtained from the present calculation for fixed boundary conditions are compared with the FLUENT code [4]. For the integral calculations presented in the following sections, nucleate boiling heat transfer coefficient of Eq.(12) will be applied with water temperature of 400 K. However, in this part, constant temperature boundary condition of 400 K is imposed on the vessel outer wall for computational simplicity to focus only on the accuracy of the present 3D conduction calculation inside the vessel wall. On the vessel inner wall, constant heat flux boundary condition from Fig. 2 is applied

Number of total nodes is 62,920 with 40 in the radial direction, 960 in the polar angle direction of the hemispherical part and 613 in the axial direction of the cylindrical part. On the other hand, the number of meshes used in the FLUENT calculation is 135,894. As noted earlier, it is assumed that the reactor vessel is solid state even though temperature is partially increased beyond its melting temperature.

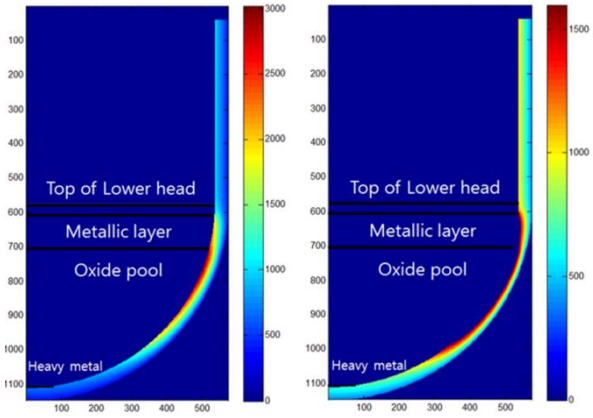

(a) Overall region (b) Un-molten region

Fig. 5. Vessel temperature contours.

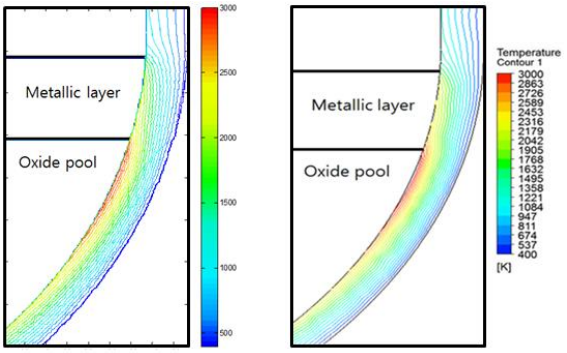

(a) Present (b) FLUENT

Fig. 6. Comparison of vessel temperature contours.

Figure 5(a) shows the temperature contour thus obtained from the present 3D calculations. At the interface of the light metal layer and the oxide pool, the temperature is the highest and the maximum temperature obtained is 3000 K. Fig. 5(b) shows the remaining vessel thicknesses obtained by eliminating the regions with temperatures higher than 1750 K. Figure 6 indicates the vessel temperature contours from the present calculation and the FLUENT code [4] and it can be found that they are in good agreement.

3.2 Multi-Dimensional Effect of the Vessel Wall

To capture the multi-dimensional effect of the vessel wall, base case condition of a hypothetical large reactor is established in Table 2. This condition is similar to but not exactly same to any large reactor.

The effect of peak heat flux at the vessel internal surface through the light metal layer is evaluated by controlling the mass. Heat transfer coefficients used are Steinberner-Reineke correlation [11] for the oxide pool and Globe-Dropkin correlation [9] and Churchill-Chu correlation [10] for the light metal layer (see Ref. 3). For these calculations, external boiling condition is fixed at nucleate boiling to capture the separate effect inside the vessel region. The peak heat fluxes assumed through the light metallic region are 2.5 MW/m^2, 3.0 MW/m^2 and 4.0 MW/m^2.

Table 2: Base case condition for a hypothetical large reactor

Parameter	Value
Reactor vessel inner radius (m)	2.3
Reactor vessel thickness (m)	0.15
Oxide pool mass (ton)	120
Metal layer mass (ton)	30
Heavy metal mass (ton)	0.1 % of light metal
Oxide pool decay power (MW)	25
Oxide crust decay power (MW)	0
Heavy metal layer decay power (MW)	0

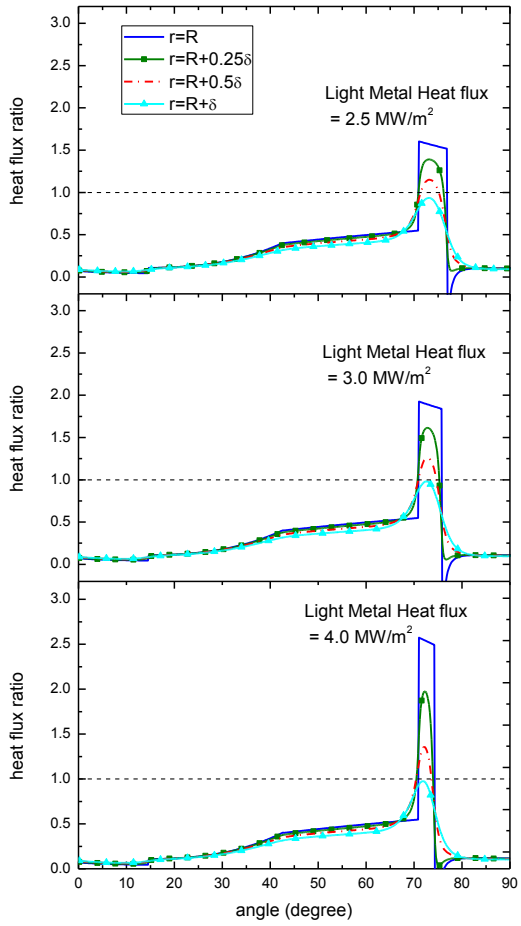

Fig. 7. Radial heat flux ratios through the vessel wall.

Figure 7 shows the radial heat flux ratios given by heat flux divided by external CHF of Eq.(14) at four radial planes of the vessel r=R, R+0.25δ, R+0.5δ and R+δ for the three cases. All the results show that the heat flux through the vessel wall is remarkably reduced from the vessel inside (r=R) to the external surface (r=R+δ) and the magnitude of the ratio at the external surface (at r=R+δ) is reduced from 1.5 to about 1.0.

This attenuation is truly due to vessel multi-dimensional heat diffusion to the lower temperature regions above and below the light metal region. For the peak heat flux of 2.5 MW/m^2 the peak heat flux ratios at the inner and outer vessel wall are 1.6 and 0.93, respectively. For 3.0 MW/m^2, they are 1.92 and 0.98. For 4.0 MW/m^2, they are 2.57, 0.98. From these results, we can figure out that the heat flux at the vessel outer wall can go below CHF due to multi-dimensional heat diffusion through massive reactor vessel wall even though internal heat flux from the metal layer is far larger than the CHF. Also, the external heat flux itself is not very sensitive to internal heat flux magnitude.

Figure 8 shows the remaining vessel wall thicknesses for the three cases after eliminating the nodes above 1750 K. The maximum ablation thickness for the three cases is about 12 cm and it can be found that the thickness is not sensitive to the peak heat flux from the light metal region.

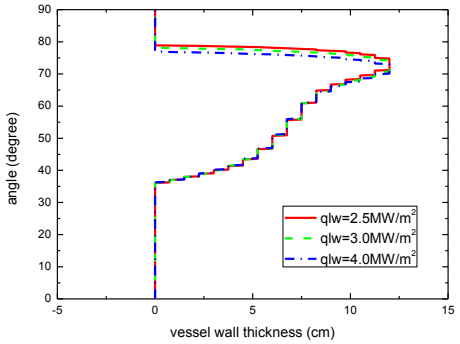

Fig. 8. Effect of light metal heat flux on vessel wall remaining thickness.

4. Conclusion

Three-layer corium model is setup and conjugate heat transfer through the reactor vessel with internal polar angle dependent heat flux and outer boiling conditions are solved for several IVR conditions. It is found that even though the internal heat flux from the metal layer goes far beyond critical heat flux the heat flux from the outer surface of the vessel can be maintained below critical heat flux. This is because the vessel can strongly diffuse the local focusing heat load from the metal layer. The conjugate heat transfer with multi-dimensional heat diffusion has been neglected in the previous studies and thus the present approach can provide promising insight for the future applications especially for large power reactors. For plant specific calculations in the future, more realistic model for reactor vessel ablation above the melting temperature and the external boiling heat transfer for the downward facing hemisphere should be needed.

Acknowledgements

This research was supported partly by a grant from the Nuclear Safety Research Program of the Korea Radiation Safety Foundation (Grant Code: 1305008-0113-HD120) and partly by the National Research Foundation of Korea (NRF) grant funded by the MSIP (No. 2012M2A8A4025897).

REFERENCES

[1] T. Theofanous, C. Liu, S. Additon, S. Angelini, O. Kymaäläinen, In-vessel coolability and retention of a core melt, Nuclear Engineering and Design, Vol.169, pp.49-57, 1997.
[2] H. Esmaili, M. Khatib-Rahbar, Analysis of In-Vessel Retention and Ex-Vessel Fuel Coolant Interaction for AP1000, Energy Research, Inc.,

NUREG/CR-6849, ERI/NRC-04-201, 2004.
[3] Y. P. Zhang, S. Z. Qiu, G. H. Su, W. X. Tian, Analysis of safety margin of in-vessel retention for AP1000, Nuclear Engineering and Design, Vol. 240, pp.2023-2033, 2010.
[4] ANSYS Inc., ANSYS FLUENT 14.0: User's Guide, 2011.
[5] W. M. Rohsenow, A Method of Correlation Heat Transfer Data for Surface Boiling of Liquids, Transaction of ASME, Vol. 74, pp.969-976, 1952.
[6] Mathworks, Inc., MATLAB Optimization Toolbox, 2013.
[7] F. P. Incropera, D. P. Dewitt, T. L. Bergman, A. S. Lavine, Introduction to heat Transfer, John Wiley & Sons, pp.73-74, 2007.
[8] J. M. Bonnet, J. M. Seiler, Thermal hydraulic phenomena in corium pools: The BALI Experiment, 7th International Conference on Nuclear Engineering, Tokyo, Japan, 1999.
[9] S. Globe, D. Dropkin, Natural Convection Heat Transfer in Liquid Confined by Two Horizontal Plates and Heated from Below, Transactions of ASME, Vol 81, pp.24-28, 1959.
[10] S.W Churchill, H. H. Chu, Correlating equations for laminar and turbulent free convection from vertical plate, International Journal of Heat and Mass Transfer, Vol.18, pp.1323-1329, 1975.
[11] U. Steinberner, H. H. Reineke, Turbulent buoyancy convection heat transfer with internal heat sources, Proceedings 6th International Heat Transfer Conference, Toronto, Canada, 1978.